CHIN. PHYS. LETT. Vol. 28, No. 2 (2011) 024202

A Full-Duplex Radio-over-Fiber System Based on Frequency Twelvefold *

ZHU Jia-Hu(朱家胡), HUANG Xu-Guang(黄旭光)**, TAO Jin(陶金), XIE Jin-Ling(谢金玲)

Key Laboratory of Photonic Information Technology of Guangdong Higher Education Institutes, South China Normal University, Guangzhou, 510006

(Received 3 November 2010)

A full-duplex radio-over-fiber system using frequency-twelvefold optical millimeter-wave based on external modulation via a Mach–Zehnder modulator is proposed and analyzed theoretically. The simulation results show that the power penalties for both the downstream and upstream signals are less than 0.5 dB. In this scheme, the configuration of a base station is simplified without laser, while the frequency of local oscillator signal is largely reduced due to the frequency-twelvefold millimeter-wave technique. The cost of the new system is largely reduced.

PACS: 42.79.Hp, 42.79.Sz. DOI: 10.1088/0256-307X/28/2/024202

In order to provide broadband, capacity, mobile and flexibility services, radio-over-fiber (RoF) has been a topic of research interest in the last few years. Optical millimeter-wave (mm-wave) generation is one of the key technologies in the RoF systems. Recently, several techniques have been proposed to implement mm-wave generation[1−13] such as direct modulation,[1] optical double-frequency heterodyning,[2] external optical modulation,[3] and so on. Among them, external intensity modulation is the simplest and the most accurate one, and shows great potential application for producing high-frequency (up to 40 GHz) mm-wave signals. Different modulation formats, such as optical carrier suppression, double-sideband, and single-sideband can be generated by external modulation schemes.[4−8] A low-cost base station (BS) or central office (CO) is one of the key techniques to make RoF systems be practical for commercial deployment. Some cost-effective RoF system schemes have been proposed and experimentally investigated, such as the technique for sharing single light source for both downlink and uplink signals.[9] On the other hand, the electrical components and equipments such as rf carrier generators, mixers, and synthesizers at frequencies over 40 GHz are very expensive. Thereby, a cost-effective way for optical mm-wave signal generation beyond 40 GHz is of great interest. Additionally, as the rf frequency increases, the effect of dispersion is even more pronounced and the fiber-link distance is severely limited.[10] In order to reduce the costs of the ultrahigh rf components, frequency multifold techniques such as frequency doubling and quadrupling[11] have been proposed. Nevertheless, as we know, the frequency twelvefold optical mm-wave with transmission performance has not been discussed so far. It could be significant for reducing the cost of the RoF system, compared with RoF systems based on direct ultrahigh rf oscillator and based on frequency doubling or quadrupling rf oscillator.

In this Letter, a low-cost full-duplex RoF system with frequency twelvefold based on an external modulation is proposed and numerically demonstrated for the first time. A twelvefold-frequency optical mm-wave signal generated with a $LiNbO_3$ Mach–Zehnder modulator (MZM) is theoretically analyzed. Bit-error-rate (BER) performances of both downstream and upstream signals are evaluated with BER testers.

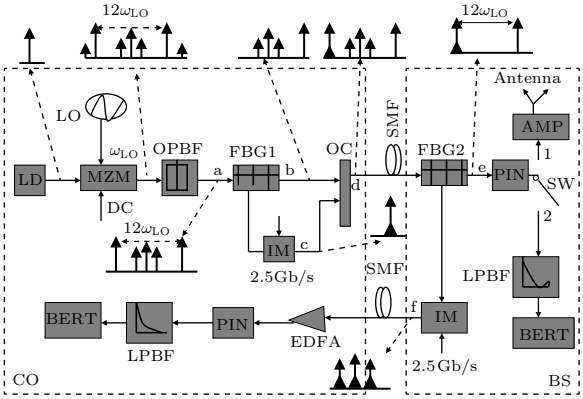


Fig. 1. The setup of the bi-directional ROF system. LD, distributed feedback laser diode; DC, direct current bias; FBG, fiber Bragg grating combining with a circulator; MZM, $LiNbO_3$ Mach–Zehnder modulator; IM, intensity modulator; OPBF, optical passband filter; OC, optical coupler; SMF, standard single-mode fiber; PIN, pin photodiode; LPBF, low passband filter; BERT, BER tester; EDFA, erbium-doped fiber amplifier; AMP, amplifier; SW, electrical switch.

Figure 1 shows the full-duplex RoF system based on an external modulation. A cw lightwave with an angle frequency ω_c is generated from a distributed feedback laser diode (LD). It can be represented as $E_c(t) = A_c \cos(\omega_c t)$. Here A_c is the lightwave field amplitude. The lightwave is intensity-modulated via a $LiNbO_3$ modulator, which is driven by two local oscillator (LO) clock signals of $V_1(t) = V_{\rm LO}\cos(\omega_{\rm LO}t)$ and $V_2(t) = V_{\rm LO}\cos(\omega_{\rm LO}t + \theta)$. Here $\omega_{\rm LO}$ and $V_{\rm LO}$ are the angular frequency and the amplitude voltage of the two LO clocks, respectively; θ is the relative phase of the clocks between the two arms of the $LiNbO_3$ modulator. Meanwhile, the direct current bias voltage V_{b1} or V_{b2} is adjusted to obtain a constant optical

*Supported by the National Natural Science Foundation of China under Grant No 61077038.

**To whom correspondence should be addressed. Email: huangxg@scnu.edu.cn

© 2011 Chinese Physical Society and IOP Publishing Ltd

phase of $\Phi_{\rm DC} = 2k\pi$ $(k = 1, 2, 3, \cdots)$ to suppress the odd-order or even-order optical sidebands.[12] According to Refs. [13,14], the output filed after the dual-arm $LiNbO_3$ modulator can be written as

$$E_{\rm out}(t) = \frac{E_c(t)}{10^{\alpha/20}}\left\{\gamma \exp\left[j\pi\frac{V_2(t)}{V_\pi} + j\pi\frac{V_{b2}}{V_\pi}\right] + (1-\gamma)\exp\left[j\pi\frac{V_1(t)}{V_\pi} + j\pi\frac{V_{b1}}{V_\pi}\right]\right\}. \quad (1)$$

where V_{b1} and V_{b2} are respectively the bias voltages of the two arms, and V_π is the half-wave voltage of the modulator; γ is the power splitting ratio of the two arms of the MZM; α is the extra insertion loss of the $LiNbO_3$ modulator. For a good $LiNbO_3$ modulator, power splitting ratio is about 0.5 and the extra loss is approximately zero. Because the components of the optical spectrum depend on the bias voltages and the relative phase θ, one can adjust them to generate optical mm-waves with different spectra. From Eq. (1), the output filed can be written as

$$E_{\rm out} = \frac{E_c}{2}\{\cos[\omega_0 t + m\cos(\omega_{\rm LO}t + \theta) + \varphi_2] + \cos[\omega_0 t + m\cos(\omega_{\rm LO}t) + \varphi_1]\}, \quad (2)$$

Here $m = \pi V_{\rm LO}/V_\pi$ is the phase modulation index and $\phi_1 = \pi V_{b1}/V_\pi$ and $\phi_2 = \pi V_{b2}/V_\pi$ are respectively constant phase shifts that are respectively induced by the dc bias voltages V_{b1} and V_{b2}.

When the relative phase is set to be $\theta = \pi$ and both the bias voltages of the $LiNbO_3$ modulator are set to be $V_{b1} = V_{b2} = 0$, it gives $\cos(2n\theta) = 1$, $\sin(2n\theta) = 0$, $\cos[(2n-1)\theta] = -1$, $\sin[(2n-1)\theta] = 0$, $\phi_1 = 0$ and $\phi_2 = 0$. Expanding Eq. (2) by using Bessel functions, the expression of the electrical filed at the output of the MZM becomes

$$E_{\rm out} = E_c\cos\omega_0 t\left[J_0(m) + 2\sum_{n=1}^{\infty}(-1)^n J_{2n}(m)\cos(2n\omega_{\rm LO}t)\right]. \quad (3)$$

Equation (3) shows that the odd-order optical sidebands are suppressed. Given an optical pass-band filter which can suppress seventh and higher-order sidebands, the Bessel function higher than $J_6(m)$ can be ignored, and one has

$$\begin{aligned} E_{\rm out} = E_c J_0(m)\{&\cos(\omega_0 t) \\ &- 2E_c J_2(m)[\cos(\omega_0 t + 2\omega_{\rm LO}t) + \cos(\omega_0 t - 2\omega_{\rm LO}t)] \\ &+ 2E_c J_4(m)[\cos(\omega_0 t + 4\omega_{\rm LO}t) + \cos(\omega_0 t - 4\omega_{\rm LO}t)] \\ &- 2E_c J_6(m)[\cos(\omega_0 t + 6\omega_{\rm LO}t) + \cos(\omega_0 t - 6\omega_{\rm LO}t)]\}. \end{aligned} \quad (4)$$

According to Eq. (4), the mm-wave signal has only the zero, the second, the fourth and the sixth-order sidebands. From the table for Bessel functions of the first kind, one can obtain that for $m = 7.32$, $J_6(7.32) = 0.352091$, $J_0(7.32) = 0.28651$ and $J_2(7.32) = -0.26244$, but $J_4(7.32) = 0.0726926$. Thus, the modulation voltage of $V_{\rm LO} = 13.99\,{\rm V}$ should be chosen to achieve the value of $m = \pi V_{\rm LO}/V_\pi = 7.32$, given a half-voltage of $V_\pi = 3\,{\rm V}$. Meanwhile, the fourth-order sidebands are suppressed. Therefore, the mm-wave with twelve times frequency of the local oscillator can be generated in this way.

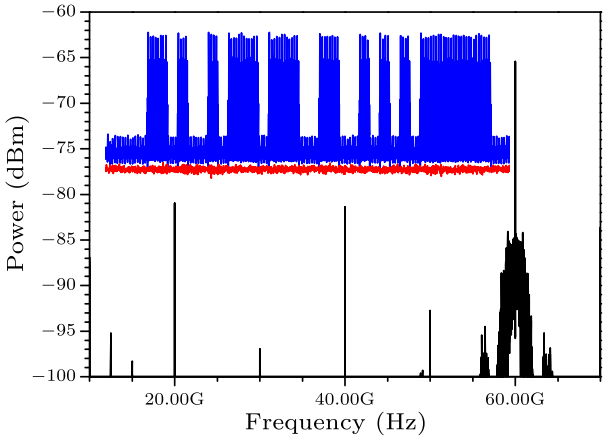


Fig. 2. Radio-frequency signal in frequency domain. Inset: rf signal in time domain.

The simulated experimental setup for the full-duplex RoF system based on an external modulation and frequency twelvefold optical mm-wave signal generation by using a $LiNbO_3$ modulator is shown in Fig. 1. In the center office, a cw lightwave with a linewidth of 10 MHz is generated from an LD with a power of 5 dBm at 1552.5 nm (193.1 THz). Optical mm-wave with 60 GHz frequency is produced via a $LiNbO_3$ modulator with 30 dB extinction ratio ($\gamma = 0.48$) and 5 dB insertion loss, which is driven by a sinusoidal wave with the frequency $\omega_{\rm LO}$ of 5 GHz. Both half-voltage V_π and the switching bias voltage are 3 V. The modulation voltage $V_{\rm LO}$ and the bias voltages of the two arms V_{b1} and V_{b2} are respectively 13.99 V, 0 V and 0 V. For the sake of comparison, all parameters mentioned above are kept the same as the theoretical analysis. The optical passband filter with a bandwidth of 78 GHz and the modulation depth of −20 dB is used to suppress the unwanted higher-order sidebands. After the MZM, the odd-order optical sidebands are suppressed, as expected from Eq. (3). The mm-wave signal has only the zero, the second, the fourth and the sixth-order sidebands after the optical passband filter from the simulation (shown in Fig. 3(a)), as expected from Eq. (4). Additionally, from Fig. 3(a) one can see that the two fourth-order sidebands are suppressed. Therefore the simulation results are in good agreement with the theoretical results. The frequency spacing between the two sixth-order sidebands is 60 GHz. Then the upper sixth-order sideband is reflectively separated by using FBG1 with the Bragg wavelength of 1552.28 nm and the bandwidth of 0.2 nm combining with a circulator. The sep-

arated upper sixth-order sideband is then modulated with a 2.5 Gb/s electrical data in a pseudorandom bit sequence length of $2^{31}-1$ by an intensity modulator. An optical coupler is used to combine the modulated sideband and the unmodulated sidebands into the long-distance SMF-28 fiber. In order to compensate for the power difference of 4.3 dB between the lower and upper sixth-order sidebands, the coupling ratio around 3 : 7 is used to achieve nearly equal amplitudes for the two sixth-order sidebands after the combination. After transmitting over the 50 km standard SMF-28 fiber with a dispersion of 17 ps·nm^{-1}·km^{-1}, at the base station, the zero and two second-order sidebands are synchronously separated from the mm-wave by using FBG2 with the Bragg wavelength of 1552.5 nm and the bandwidth of 0.28 nm combining with a circulator. The separated zero and two second-order sidebands are remodulated with a 2.5 Gb/s upstream data, are transmitted over another 50 km fiber, and arrive at the central office. After the PIN, the optical mm-wave signal is converted into an electric mm-wave with 60 GHz frequency. The electric mm-wave is then amplified and finally broadcasted via the antenna, when the rf signal is switched to output 1 of the electrical switch (SW). Figure 2 shows the rf signal in time-domain and frequency-domain after the PIN. It can be clearly seen that the rf signal includes a 60 GHz carrier modulated with a 2.5 Gbit/s digital data (or information). The optical spectra measured at points a, b, c, d, e and f are shown in Figs. 3(a), 3(b), 3(c), 3(d), 3(e) and 3(f), respectively.

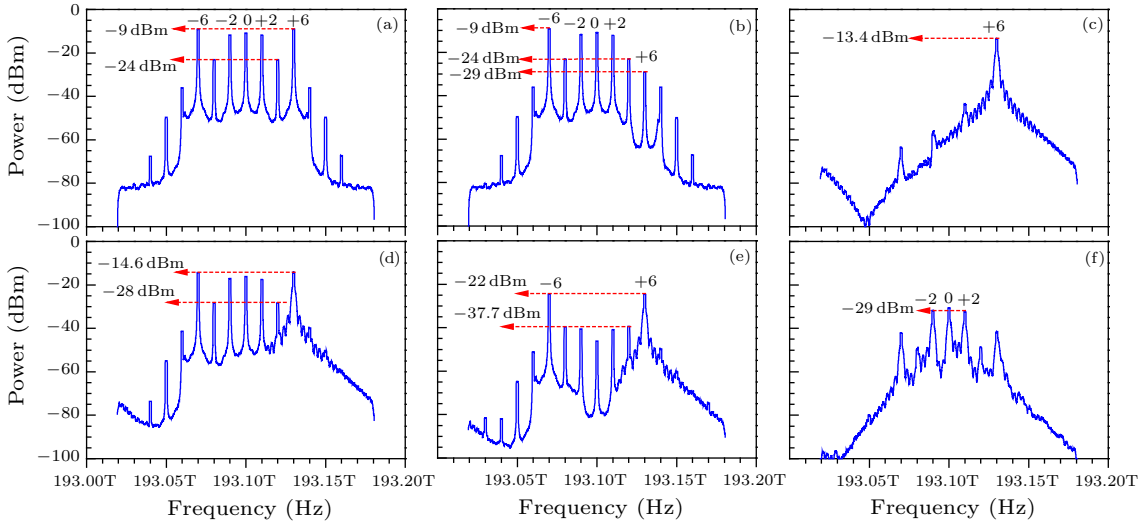


Fig. 3. Optical spectra at different locations. (a) Optical spectrum after passing through the optical filter; (b) optical spectrum of the unmodulated signals; (c) optical spectrum modulated by 2.5 Gbit/s data; (d) optical spectrum after an OC; (e) optical spectrum of mm-wave; (f) optical spectrum remodulated by 2.5 Gbit/s upstream data.

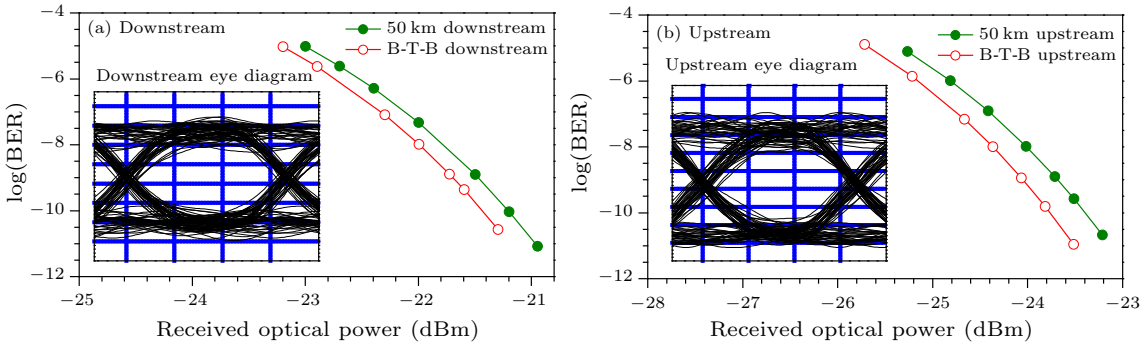


Fig. 4. BER curves for both downstream data and upstream data. The upstream signals are amplified by an EDFA with the gain of 12 dBm. Insets: for both downstream and upstream eye diagrams.

The BER performances for both downlink and uplink are measured after they are filtered with low pass-band filters (LPBF) with the bandwidth of 2 GHz. Figures 4(a) and 4(b) show the BER curves of the downlink data and uplink data, respectively. Both for downlink data and uplink data, after transmitting over 50 km, the power penalties are less than 0.5 dB at a given BER of 10^{-9}. The insets of Fig. 4 illustrate the eye diagrams of the downstream and upstream signals transmitted over 50 km. One can see that the eye diagrams are still wide open after 50 km distance transmission. Hence, the new system is suitable for long distance transmission.

A comparison between the double-band data-modulating (DBDM) used in the conventional carrier-suppressed double sideband system and the single-

band data-modulating (SBDM) used in the proposed system is shown in Fig. 5. Figure 5 shows the eye diagrams of the baseband signals based on the method modulating the data into two sidebands after 0, 20 and 40 km transmissions and based on the method modulating the data into single sideband after 20, 40 and 60 km transmissions, respectively. From the eye diagrams, it can be seen that the SBDM has better performances than DBDM. The simulation result shows that the longest transmission distance of the signal in the DBDM-based conventional system with 60 GHz carrier frequency is limited to 40 km. The longest transmission distance in the SBDM-based frequency-twelvefold system, however, exceeds to 40 km. It means that the proposed scheme can be immunized the fading effect, the time shift of the code and the walk-off of signals.

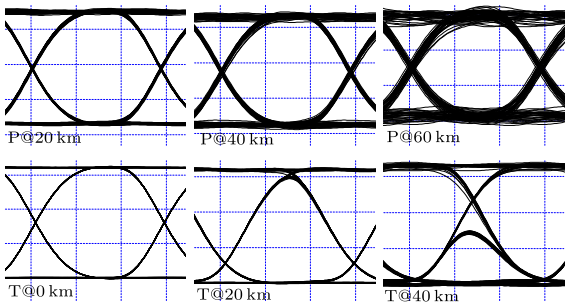


Fig. 5. The eye diagrams of the baseband signals in the SBDM-based frequency-twelvefold system after 20, 40 and 60 km transmissions (upper diagrams) and in the DBDM-based conventional system after 0, 20 and 40 km transmissions (lower diagrams), respectively.

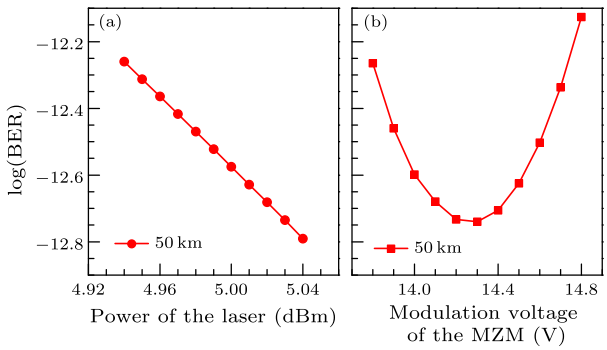


Fig. 6. (a) The variation of the BER caused by the power fluctuation of the laser diode. (b) The variation of the BER caused by the deviation of the modulation voltage of the MZM.

In order to learn the feasibility and stability of the system, we perform parametric sensitivity studies for various key-component specification tolerances such as the power of the laser diode, the modulation voltage and the extinction ratio (or splitter ratio γ) of the Mach–Zehnder modulator. Characteristic parameters of all of the components in the system are chosen based on their typical specifications of real products. In the simulation, noises such as signal-ASE noise, ASE-ASE noise, thermal noise and shot noise are also included into the pin photodiode. Figure 6(a) shows the variation of the BER caused by the power instability of the laser diode. One can see that the instability of the laser diode only induces a little alteration of the BER. The influence of the deviation of the modulation voltage of MZM on the BER is shown in Fig. 6(b). One can see that the deviation of the modulation voltage of the MZM only causes a little degradation of the BER. The simulation also shows that the influence of the extinction ratio of the MZM on the BER can be ignorable. The sensitivity analysis reveals that the system has not tiny specification tolerances for the laser diode and the MZM.

In conclusion, a full-duplex radio-over-fiber system that can generate twelvefold-frequency based on an external modulation is proposed and numerically demonstrated. The optical mm-wave generated via a $LiNbO_3$ modulator is theoretically analyzed. The simulation results show that the power penalties for both the downstream and upstream signals are less than 0.5 dB. In this scheme, the configuration of a base station is simplified without laser. Additionally, the frequency of LO signal is largely reduced because frequency twelvefold mm-wave is employed. Hence, the cost of the new system is largely reduced.

References

[1] Jaro G and Berceli T 2003 *J. Lightwave Technol.* **21** 3078
[2] Wake D, Lima C R, and Davies P A 1996 *IEEE Photon. Technol. Lett.* **43** 2270
[3] Yu J, Jia Z, Wang T and Chang G K 2007 *IEEE Photon. Technol. Lett.* **19** 1499
[4] Smith G H, Novak D and Ahmed Z 1997 *IEEE Trans. Microwave Theory. Technol.* **45** 1410
[5] Attygalle M, Lim C, Pendock G J, Nirmalathas A and Edvell G 2005 *IEEE Photon. Technol. Lett.* **17** 190
[6] Fuster J M, Marti J, Corral J L, Polo V and Ramos F 2000 *J. Lightwave Technol.* **18** 933
[7] Sun C K, Orazi R J and Burns W K 1996 *IEEE Photon. Technol. Lett.* **8** 154
[8] Kojucharow K, Sauer M, Kaluzni H, Sommer D, Poegel F, Nowak W, Finger A and Ferling D 1999 *IEEE Trans. Microwave Theor. Technol.* **47** 2249
Kur T, Kitayama K and Takahashi Y 1999 *MWP '99. International Topical Meeting on Microwave Photonics* 123
[9] Schmuck H 1995 *Electron. Lett.* **31** 1848
[10] Zhu J H, Huang X G and Xie J L 2011 *Opt. Commun.* **284** 729
[11] Qi G, Yao J, Seregelyi J, Paquet S, Zhang X, Wu K and Kashyap R 2006 *IEEE J. Lightwave. Technol.* **24** 4861
[12] Cartledge, J C, Rolland C, Lemerle S and Solheim A 1994 *IEEE Photon. Technol. Lett.* **6** 282
[13] Cartledge J C 1995 *IEEE Photon. Technol. Lett.* **7** 1090